Journal of Medicinal Chemistry Article

J. Med. Chem. **2010,** *53,* 2865–2874 **2865**
DOI: 10.1021/jm901823u

In Vitro and In Vivo Photocytotoxicity of Boron Dipyrromethene Derivatives for Photodynamic Therapy

Siang Hui Lim,[†] Cliferson Thivierge,[‡] Patrycja Nowak-Sliwinska,[§] Junyan Han,[‡] Hubert van den Bergh,[§] Georges Wagnières,[∥] Kevin Burgess,[‡] and Hong Boon Lee*,[†]

[†]*Cancer Research Initiatives Foundation (CARIF), Sime Darby Medical Centre, 47500 Subang Jaya, Selangor, Malaysia,* [‡]*Department of Chemistry, Texas A&M University, College Station, Texas 77842,* [§]*Institute of Bio-Engineering, and* [∥]*Institute of Chemical Sciences and Engineering, Medical Photonics Group, Swiss Federal Institute of Technology (EPFL), 1015 Lausanne, Switzerland*

Received December 10, 2009

To understand the effects of substitution patterns on photosensitizing the ability of boron dipyrromethene (BODIPY), two structural variations that either investigate the effectiveness of various iodinated derivatives to maximize the "heavy atom effect" or focus on the effect of extended conjugation at the 4-pyrrolic position to red-shift their activation wavelengths were investigated. Compounds with conjugation at the 4-pyrrolic position were less photocytotoxic than the parent unconjugated compound, while those with an iodinated BODIPY core presented better photocytotoxicity than compounds with iodoaryl groups at the meso-positions. The potency of the derivatives generally correlated well with their singlet oxygen generation level. Further studies of compound **5** on HSC-2 cells showed almost exclusive localization to mitochondria, induction of G_2/M-phase cell cycle block, and onset of apoptosis. Compound **5** also extensively occluded the vasculature of the chick chorioallantoic membrane. Iodinated BODIPY structures such as compound **5** may have potential as new photodynamic therapy agents for cancer.

Introduction

Photodynamic therapy (PDT[a]) is now a well-recognized modality for cancer treatment, but to date, only a small number of PDT drugs, namely, porfimer sodium, temoporfin, and aminolevulinic acid, have been approved mainly for treatment of skin, gynecological, gastrointestinal, and some head and neck cancers.[1] PDT involves site-specific activation of an administered photosensitizer using light of a wavelength matched to the λ_{max} of the photosensitizer[2,3] in order to generate cytotoxic reactive oxygen species (e.g., $^1O_2$) that eradicate tumors via cellular damage, via vasculature damage or by recruiting members of the inflammatory and immune response system.[2,3] These photosensitizers, as well as the majority of those currently being investigated in clinical trials, share a common cyclic tetrapyrrole structure,[4] probably due to the fact that modern PDT has evolved from naturally derived porphyrins such as hematoporphyrin. Aside from cyclic tetrapyrrole structures, a number of naturally occurring and synthetic dyes that are non-porphyrin have also been evaluated for their photosensitizing ability against cancer. The focus has been primarily on cationic structures such as methylene blue, Nile blue, and Nile red analogues and the chalcogenopyrylium class of photosensitizers. These classes of compounds, however, suffer from a major drawbacks due to their inherent dark cytotoxicity.

One alternative class of non-porphyrin photosensitizers that has emerged recently is the BODIPY chromophore. BODIPYs have many characteristics of an ideal photosensitizer including high extinction coefficients, high quantum efficiencies of fluorescence, relative insensitivity to environment, and resistance to photobleaching. Nagano and co-workers reported the synthesis of a simple diiodo-substituted BODIPY with possible applications that included PDT. The diiodo-substituted BODIPY at the 4-pyrollic position produces the supposed internal heavy atom effect and subsequently enhanced the intersystem crossing efficiency from a singlet to a triplet state that controls the singlet oxygen production.[5] O'Shea and co-workers prepared a series of azadipyrromethenes with high absorption in the far-red wavelengths and demonstrated their efficacy in light-induced toxicity in a panel solid tumor cell line.[6] One of the azadipyrromethenes was later shown to effectively eradicate the subcutaneously xenografted MDA-231 breast tumors in nude mice.[7] Akkaya and co-workers introduced another class of water-soluble BODIPY dyes with extended conjugation at the 5-pyrollic positions.[8] These photosensitizers were shown to have strong absorptions in the 650−680 nm therapeutic window and good photoinduced cytotoxicity in K562 leukemia cells at submicromolar concentrations even under low fluence rate LED irradiation.

*To whom correspondence should be addressed. Phone: +603-5639-1874. Fax: +603-5639-1875. E-mail: hongboon.lee@carif.com.my.

[a] Abbreviations: BODIPY, boron dipyrromethene; PDT, photodynamic therapy; CAM, chorioallantoic membrane; EDD, embryo development day; Rh123, rhodamine 123; DPBF, 1,3-diphenylisobenzofuran; MTT, methylthiazolyldiphenyltetrazolium bromide; DMSO, dimethyl sulfoxide.

© 2010 American Chemical Society

Published on Web 03/03/2010

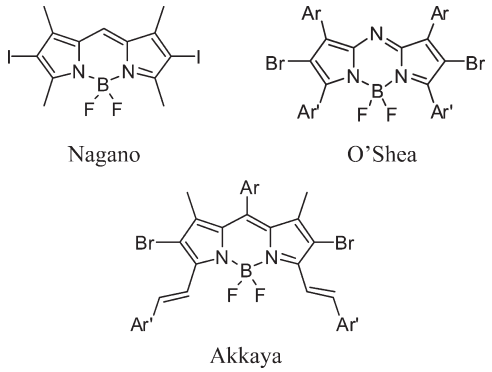

This study investigates the effects of two structural variations of BODIPY on their photocytotoxicity in terms of photophysical properties and in vitro and in vivo efficacies. In the first variation, functionalizations such as meso-substitution and sulfonation to improve hydrophilicity were tested to fine-tune the activity of iodinated BODIPY-based structures such as Nagano's compound (**6** in Figure 1). Because photosensitizers that absorb in the longer wavelengths may be activated deeper in the tissues and may therefore be clinically favored, a second variation consisting of compounds with extended conjugation at the 4-pyrollic position, which is a structural variation that has not been studied prior to this, was included in this study. First, the PDT efficacy of these BODIPY-based photosensitizers on a panel of leukemia and solid tumor cell lines, with particular attention on their structure−activity relationships, was studied. The effect of the most active derivative on an oral cancer cell line, HSC-2, was further investigated for intracellular localization, cell cycle arrest, and onset of apoptosis experiments, as well as in a preclinical in vivo model using the chick chorioallantoic

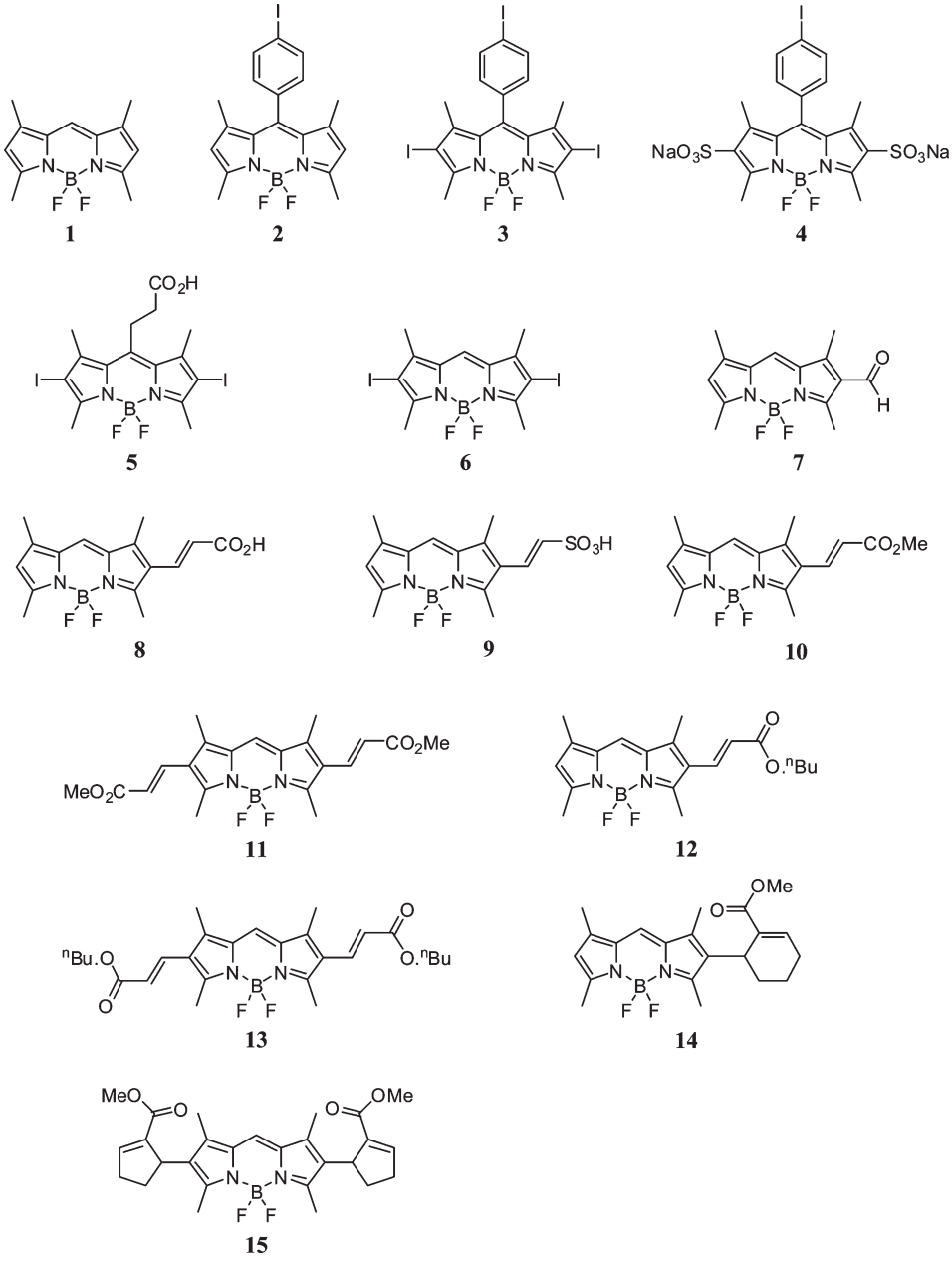

Figure 1. Structures of BODIPY.

membrane (CAM), in ovo, for PDT efficacy in terms of vascular occlusion.[9]

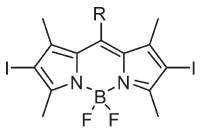

Structural variation 1

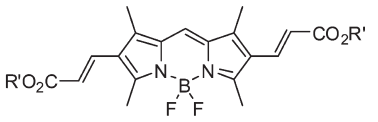

Structural variation 2

Results and Discussion

Structural Variations and Photophysical Properties. Two structural variations around the BODIPY core of compound **1** were investigated in this study (Figure 1). The first (compounds **2**−**6**) investigated the effectiveness of various iodinated derivatives in order to maximize the "heavy atom effect". To fine-tune the activity of iodinated BODIPY-based structures, additional functionalizations such as meso-substitution with alkyl or aryl groups as well as sulfonation to improve hydrophilicity were tested. Compound **5** contains a carboxylic acid handle and could be easily attached to other molecules later if required. For the second variation (compounds **7**−**15**), the effect of extended conjugation at the 4-pyrollic position was examined. Extended conjugation at the 4-pyrrolic positions increases the absorption wavelength of the compounds to the red, permitting the use of longer excitation wavelength that penetrates deeper into biological tissues for effective treatment.

Table 2 summarizes the photophysical data of compounds **1**−**15**. The absorption and emission wavelengths of compounds **1**−**15** range from 500 to 600 nm. As expected for compounds **8**−**15**, extending the conjugation with an acrylate shifts the $\lambda_{abs\,max}$ to the red by 20−30 nm while attaching two acrylates red-shifts the $\lambda_{abs\,max}$ by 50−60 nm, compared to compound **1**. The $\lambda_{abs\,max}$ values for iodinated compounds **3**, **5**, and **6** are also red-shifted compared to compound **1** but not for compounds **2** and **4**, which are aryl-iodinated at the meso position. In addition, all compounds have high extinction coefficients and high quantum efficiencies of fluorescence except for a few structures. Among the exceptions, compounds **3**, **5**, and **6** have much lower quantum efficiency of fluorescence and a correspondingly higher singlet oxygen generation rate (Table 3) compared to the other BODIPYs studied here, probably as a result of the enhanced intersystem crossing efficiency from the lowest singlet excited state to the triplet state contributed by the internal heavy-atom effect. As in the case of the $\lambda_{abs\,max}$ values above, compounds **2** and **4** which contain a para-iodoaryl group at the meso position did not demonstrate the same loss in fluorescence yields or the same increase in singlet oxygen generation rate as compounds **3**, **5**, and **6** probably because in the former group, first, the iodine atom is not directly attached to the BODIPY core and, second, the iodoaryl plane is twisted relative to the BODIPY plane,[10] overall causing the aryl iodine atom to only, at most, elicit an intramolecular external heavy-atom effect.[6]

In Vitro Photocytotoxic and Comparative Singlet-Oxygen Generation. The in vitro photocytotoxic activity of compounds **1**−**15** against a promyelocytic leukemia cell line (HL-60), an oral squamous carcinoma cell line (HSC-2), and a nasopharyngeal carcinoma cell line (HK1) following irradiation with 4.1 J/cm^2 of a broad spectrum light was determined using a modified methylthiazolyldiphenyltetrazolium bromide (MTT) assay. Parallel assays without light irradiation were also carried out to determine cytotoxicity in the dark. Results were expressed as IC_{50}, the concentration of compound (in μM) that inhibits proliferation rate by 50% compared to control untreated cells. The parent compound, denoted as **1**, was also prepared and tested for comparison. From the assay, all compounds had negligible or undeterminable unirradiated cytotoxicity up to 100 μM. Upon irradiation with 4.1 J/cm^2 of light, compounds **1**−**6** and **10**−**15** demonstrated photosensitized cytotoxicity with IC_{50} values in the submicromolar to tens of micromolar range. Compounds **5** and **6**, which had two iodine atoms directly attached to the BODIPY core, showed the highest activity among the analogues, with IC_{50} values that are up to 100 times lower than that of compound **1** (0.045 μM vs 4.4 μM in HL-60). In contrast, compounds **7**−**9** displayed poor activity with undeterminable IC_{50} up to 100 μM.

The influence of the iodine atom on the photocytotoxic activity of the compounds was evident from studying compounds **1**−**6**. Meso-substitution with a para-iodoaryl group in compound **2** does not alter the photocytotoxicity significantly compared to compound **1**, while further substitution with iodine atoms on the two pyrrolic 4-carbon to yield either compound **3** from **2** or compound **6** from **1** improved the activity by 10- and 100-fold, respectively, in all three cell lines, alluding to the importance of iodine atom substitution on the pyrrollic carbons rather than on the meso-aryl position. Compound **5**, which has an additional carboxylic acid

Table 1. Damage Score of PDT-Induced Vasculature Network Occlusion

occlusion score	findings
0	No occlusion
1	Partial closure of capillaries of diameter of $< 10\ \mu$m
2	Closure of capillary system, partial closure of blood vessel of diameter of $< 30\ \mu$m, and size reduction of larger blood vessels
3	Closure of vessels of diameter of $< 30\ \mu$m and partial closure of larger blood vessels
4	Total closure of vessels of diameter of $< 70\ \mu$m and partial closure of larger vessels
5	Total occlusion of vessels in the irradiated area

Table 2. Photophysical Properties of BODIPY Derivatives

compd	$\lambda_{abs\,max}$ (nm)	ε ($M^{-1}\,cm^{-1}$)	$\lambda_{em\,max}$ (nm)	Φ_{fl} [a]	ref dye[b]	solvent
1	505	83 000	516	0.80	1	EtOH
2	504	82 000	510	0.64	1	$CHCl_3$
3	537	89 000	552	0.05	2	CH_2Cl_2
4	498	100 000	509	0.34	1	H_2O
5	525	93 000	540	0.03	2	EtOH
6	534	110 000	548	0.02	1	MeOH
7	494	81 000	504	0.95	1	EtOH
8	531	27 000	570	0.42	2	EtOH
9	529	[c]	560	0.25	2	EtOH
10	527	63 000	549	0.73	2	EtOH
11	559	13 000	580	0.51	3	EtOH
12	528	62 000	551	0.73	2	EtOH
13	560	30 000	580	0.52	3	EtOH
14	517	63 000	527	0.78	2	EtOH
15	530	72 000	539	0.92	2	EtOH

[a] Φ_{fl} represents quantum efficiency of fluorescence. [b] Reference dyes used for quantum yield determination (solvent, Φ_{fl}): (1) fluorescein (0.1 M NaOH, 0.92); (2) rhodamine 6G (EtOH, 0.94); (3) rhodamine B (EtOH, 0.97). [c] Value not determined.

Table 3. Comparative Singlet Oxygen Generation and in Vitro Photo Cytotoxicity Induced by BODIPY

		activity IC_{50} (μM)[b]					
		HL-60		HSC-2		HK1	
BODIPY	singlet oxygen generation, relative rate[a]	0 J/cm^2	4.1 J/cm^2	0 J/cm^2	4.1 J/cm^2	0 J/cm^2	4.1 J/cm^2
1	0.48	> 100	4.4 ± 0.4	> 100	8.7 ± 2.0	76.8 ± 10.6	6.2 ± 1.2
2	0.15	> 100	2.7 ± 1.2	> 100	5.1 ± 0.8	> 100	5.7 ± 0.1
3	13.9	10	0.42 ± 0.06	10	0.5 ± 0.1	95.5 ± 7.9	0.69 ± 0.08
4	0.07	> 100	54.3 ± 8.3	> 100	59.4 ± 6.2	> 100	59.0 ± 7.1
5	24.6	> 100	0.045 ± 0.004	> 100	0.10 ± 0.06	55.8 ± 0.8	0.57 ± 0.1
6	23.9	> 100	0.062 ± 0.011	> 100	0.64 ± 0.06	> 100	0.57 ± 0.06
7	0.07	> 100	> 100	> 100	> 100	> 100	> 100
8	0.01	> 100	> 100	> 100	> 100	> 100	> 100
9	0.00	> 100	> 100	> 100	> 100	> 100	> 100
10	0.57	> 100	4.8 ± 0.7	> 100	5.4 ± 0.6	> 100	5.3 ± 0.6
11	0.41	> 100	5.2 ± 0.6	> 100	11.1 ± 7.4	> 100	8.5 ± 0.5
12	0.73	> 100	0.49 ± 0.07	> 100	0.6 ± 0.1	99.6 ± 0.6	1.1 ± 0.6
13	0.17	> 100	57.7 ± 6.6	> 100	37.7 ± 15.7	> 100	> 100
14	0.24	> 100	4.9 ± 0.6	> 100	4.1 ± 0.2	> 100	5.0 ± 0.6
15	0.29	> 100	3.8 ± 0.7			> 100	4.8 ± 0.9

[a] Comparative singlet oxygen generation of photosensitizers relative to methylene blue. [b] IC_{50}, the concentration of compound that inhibits the proliferation rate by 50% compared with control untreated cells. Values represent the mean ± SD of three determinations assessed 24 h using standard MTT assay. Cells were incubated with compound for 2 h prior to irradiation with 4.1 J/cm^2.

tether at the meso position, has similar to marginally better activity than compound **6** in all three cell lines. An attempt to improve the water solubility of compound **2** by substituting with sodium sulfonate to yield compound **4** resulted in 10 times loss in activity.

For the effect of extended conjugation at 4-pyrrolic positions on photocytotoxic activity of BODIPYs, compounds **7**−**15** were studied. Extending the 4-pyrollic carbon with a single aldehyde (**7**) or the hydrophilic allylic carboxylic acid (**8**) and allylic suphonic acid (**9**) resulted in loss of activity of greater than 100 μM IC_{50} values. Single extensions at the 4-pyrrolic position with acrylate esters affected the activity differently depending on the length of the alkyl ester group, where the methyl compound **10** showed no change in activity while *n*-butyl compound **12** demonstrated 10-fold improvement in activity compared to compound **1**. For compounds with double extension with the same groups at the 4-pyrollic positions, the methyl compound **11** remained unaltered in its activity compared to compound **1**, but interestingly, the *n*-butyl compound **13** showed 10-fold loss in activity compared to **1** or 100-fold loss compared to the singly extended counterpart **12**. The explanation for the reversal in structure−activity relationship of the *n*-butyl acrylate esters compared with the methyl acrylate esters from the single- to the double-extension (compounds **10** and **12** compared with compounds **11** and **13**) is not obvious and could just be due to the poorer solubility of the doubly extended *n*-butyl derivative **13**. Compounds **14** and **15**, which were failed attempts to prepare the analogous ring-constrained conjugated structures, were also tested and showed similar activities compared to compound **1**, further suggesting the minor role that 4-pyrrolic extended conjugation or the lack of it plays in modulating the photocytotoxicity of the BODIPY structures.

Subsequently, the relative rate of singlet oxygen generation was measured for compounds **1**−**15** by monitoring the reaction of known singlet oxygen acceptor 1,3-diphenylisobenzofuran (DPBF) with photosensitizers generated singlet oxygen.[11] This was achieved by following the loss of DPBF absorbance at 410 nm at an initial concentration of 50 μM over a period of 1 h. A light source filtered at 510 nm wavelength was used to minimize the photobleaching of DPBF. As a result, this would have caused an underestimation of singlet oxygen generation rate of the compounds with $\lambda_{abs\,max}$ lower than 510 nm, as the light transmission through the filter begins to drop below 510 nm. Each of the compounds was tested at an equivalent concentration of reference sensitizer methylene blue. The results from this study ranged from 0.01- to over 24-fold of singlet oxygen generation rate compared to that of methylene blue. Importantly, the rate of reactive oxygen generation measured generally correlated with the potency of these compounds and there may be a main factor affecting the photocytotoxicity of these BODIPY compounds.

Photosensitizer Cellular Localization. To ascertain the intracellular localization of the BODIPYs, compound **5**, owing to its good potency data, was chosen and examined by spinning disk confocal microscopy using dual staining techniques (Figure 2). Costaining images and topographic profiles of HSC-2 cell line loaded with compound **5** and a mitochondria-specific dye rhodamine 123 (Rh123) revealed an almost identical overlap, suggesting that compound **5** localized particularly well in mitochondria (Figure 2A,B). In comparison, compound **5** displayed only partial colocalization with endoplasmic reticulum and lysosomes, according to the confocal images and topographic profiles of compound **5** with ER-Tracker (Figure 2C,D) and with LysoTracker (Figure 2E,F), respectively. Staining of the cytoplasmic or nuclear membrane by compound **5** was not detected, indicating that it does not react nonspecifically with biological membranes. Furthermore, the nucleus remained free of compound **5** (dark nuclear area), signifying that this class of compounds would not be expected to directly damage DNA.

Mitochondria perform vital cellular functions and are involved in multiple signaling cascades in regulation of metabolism, cell cycle control development, and cell death.[12] In PDT, mitochondria are an important target. During mitochondria-photosensitization in PDT, cytochrome *c* is released from mitochondria to directly effect rapid cell death

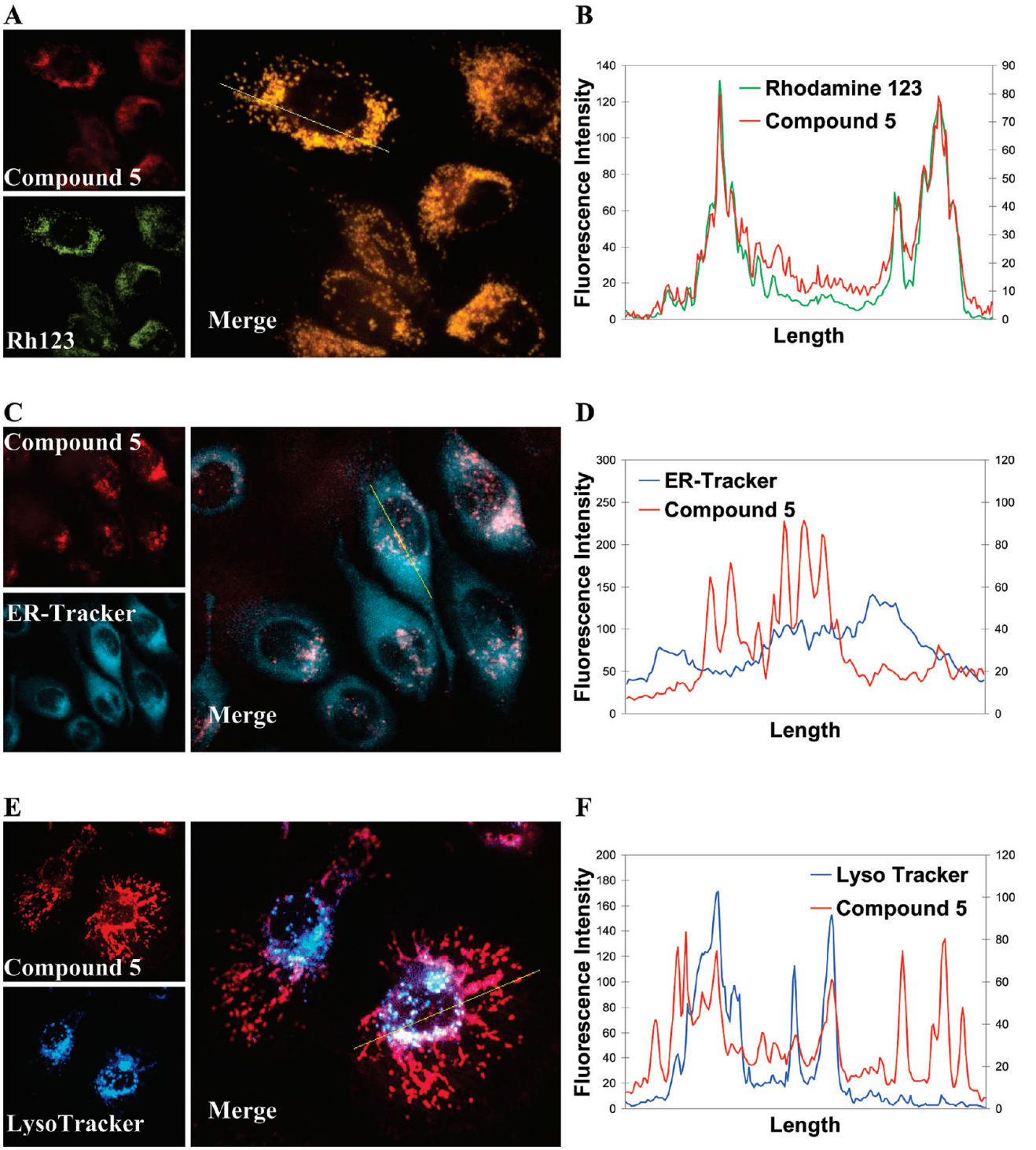

Figure 2. Intracellular localization of compound **5** in HSC-2 cells. Spinning disk confocal images (A, C, E) and fluorescence topographic profiles (B, D, F) of HSC-2 cells double-stained with 100 nM compound **5** and respective organelle probes. (A, B) Mitochondria were labeled with 100 nM Rh123 and excited at 494 nm. (C, D) Endoplasmic reticulum were labeled with 100 nM ER-Tracker and excited at 365 nm. (E, F) Lysosomes were labeled with 500 nM of LysoTracker and excited at 365 nm. Compound **5** was excited at 575 nm. Line indicates the longitudinal transcellular axis analyzed to generate the topography fluorescence profiles. Objective magnification is ×63.

through downstream effector pathways of apoptosis, bypassing other upstream apoptotic signaling pathways that require synthesis of new proteins. This mechanism of action is particularly useful in the treatment of cancer types that are chemoresistant because of mutations in upstream pro-apoptotic signaling pathways.[13]

Cell Cycle Arrest and Apoptosis. To study the mechanism of action of compound **5** that contributed to its photocytoxicity, the effect of compound **5** on cell cycle and apoptosis of HSC-2 cells was investigated using flow cytometric method. The cell cycle profile of HSC-2 cells treated with compound **5** was analyzed in a time course experiment. At 0.25 μM, compound **5** was found to induce G_2/M arrest in HSC-2 cells as early as 2 h following light irradiation (Figure 3). HSC-2 cells in G_2/M phase gradually increased from 26.1% in the control group to 39.8%, 48.4%, 55.5%, respectively, at 2, 4, and 6 h after light

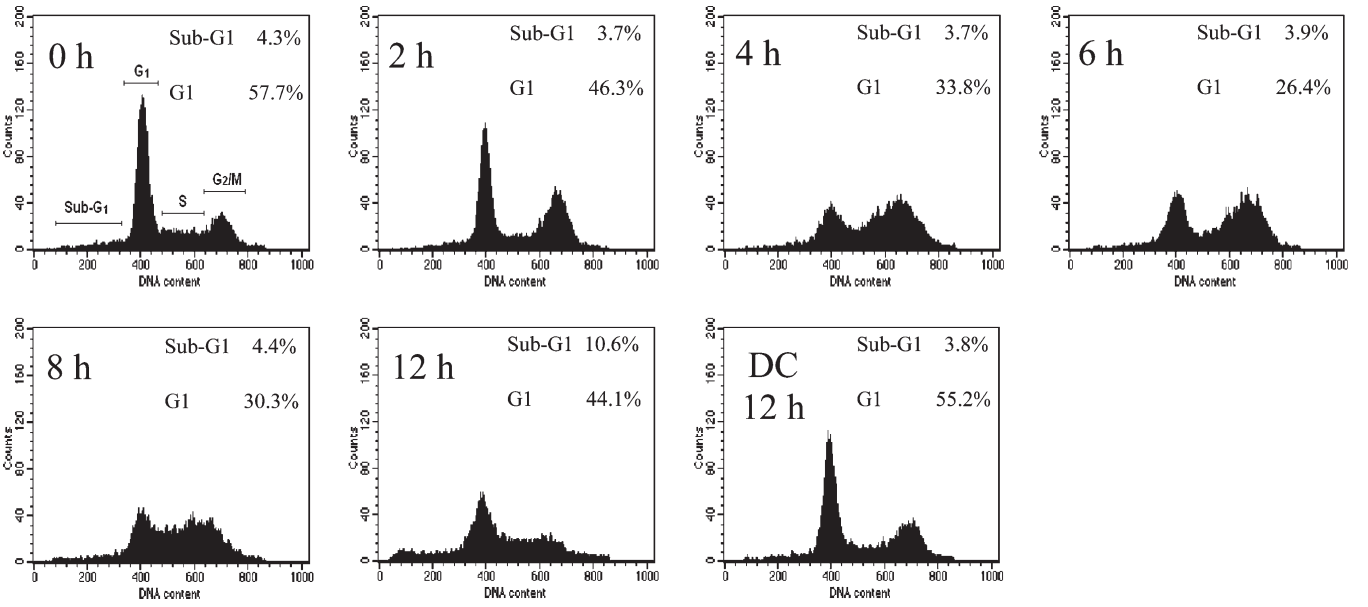

Figure 3. Effects on HSC-2 cell cycle phase at various intervals postirradiation analyzed using flow cytometry after treatment with 0.25 μM compound **5** and irradiated with a light dose of 4.1 J/cm^2. DC represents unirradiated dark control.

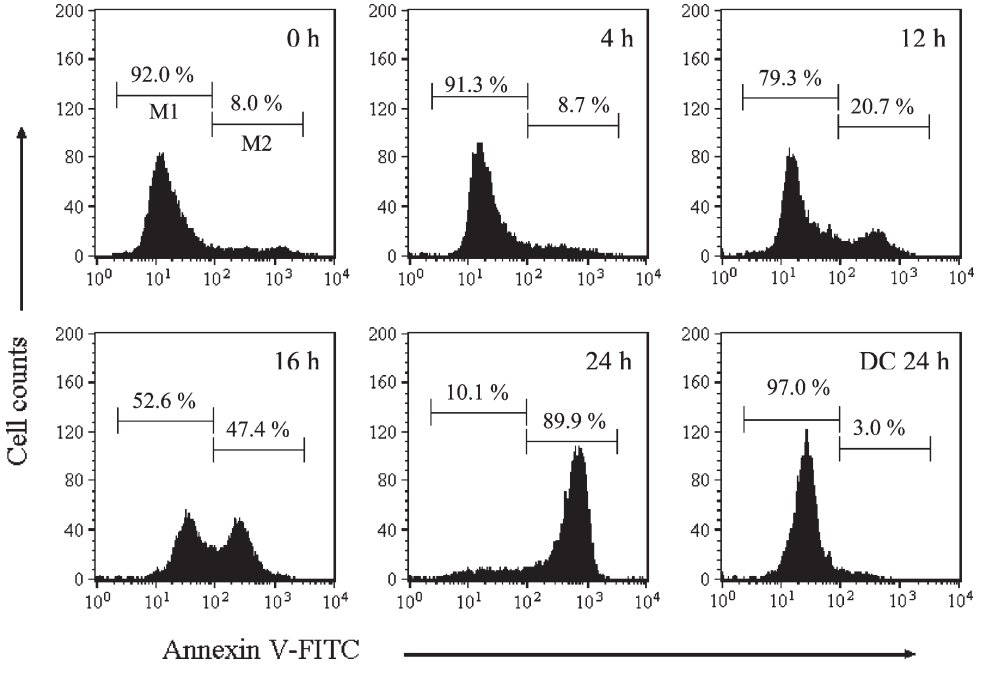

Figure 4. Representative histograms of the event of annexin V−fluorescein isothiocyanate (FITC) binding to phosphatidylserine as an indicator of apoptosis in HSC-2 cells treated with 0.5 μM compound **5** and irradiated with a light dose of 4.1 J/cm^2. M1 represents viable cell population, M2 represents apoptotic cell population, and DC represents unirradiated dark control.

irradiation. Concomitant with the increased proportion of G_2/M phase cells, HSC-2 cells in the G_1 phase were reduced from 57.7% to 46.3%, 33.8%, and 26.4% while the proportion of HSC-2 cells in S phase remained fairly constant. At 8 and 12 h, the proportion of cells arresting in the G_2/M phase was reduced to 48.8% and 26.0%, respectively, after light irradiation. Following the reduction of the proportion of cells arresting in G_2/M phase, an increase of sub-G_1 cells population from 8 to 12 h (from 4.4% to 10.6%) was observed. The proportion of cells treated with compound **5** without irradiation remains unchanged compared to control.

In the present study, the maximal level of G_2/M cell-cycle arrest was observed at 6 h after PDT. Thereafter, the recovery of the cell cycle profile to one with a reduced G2/M peak may be due to the redistribution of cells to sub-G_1, indicating the onset of apoptosis of arrested cells. A similar G_2/M arrest was also observed in hypericin-based PDT, a naturally occurring photosensitizer currently undergoing research.[14,15] Photosensitization of Hela cervical cancer cells with hypericin resulted in phosphorylation of mitochondria Bcl-2 that correlated with G_2/M cell cycle arrest, followed by the onset of apoptosis.[14]

In addition to cell cycle analysis, the onset of apoptosis was also quantified in flow cytometry experiments by measuring the externalization of membrane phosphatidylserine through annexin V−FITC staining, an event that is

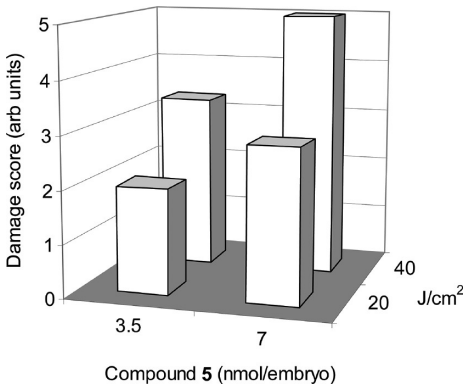

Figure 5. Effects of drug concentration and light dose on vascular occlusion efficacy of compound **5** in the CAM model. Error bars represent standard error mean from at least 10 embryos.

considered characteristic of cells undergoing apoptosis (Figure 4). Flow cytometric analysis of HSC-2 cells treated with 0.5 μM compound **5** showed the onset of apoptosis by 12 h following irradiation with 20.7% of the cells stained positive for annexin V compared to less than 10% at 0 or 4 h time points. The proportion of cells undergoing apoptosis continued to increase rapidly to 47.4% by 16 h, and at 24 h the apoptotic cell proportion was at 89.9%.

PDT-Induced Vascular Occlusion. One of the ways PDT causes damage during cancer treatment is by shutdown of blood vessels feeding the tumor.[16] Hence, the ability of compound **5** to exert in vivo vasculature disruption was investigated using the in ovo CAM model. In the present study, the ability of compound **5** to induce occlusion of blood vessels in the CAM by PDT was performed at 3.5−7.0 nmol/embryo with a light dose of 20−40 J/cm^2. The degree of vascular occlusion was scored 24 h after treatment according to Table 1. The score for photosensitizer-mediated PDT-induced vascular occlusion is shown in Figure 5, and the angiograms representing the vascular occlusion score are shown in Figure 6. As expected, the degree of vascular occlusion increased with drug and light dose. The average CAM vasculature damage score when irradiated at 20 J/cm^2 on embryos treated with 3.5 and 7.0 nmol/embryo of compound **5** was at approximately 2 and 3, respectively. When the light dose increased to 40 J/cm^2, the damage score increased accordingly to 3.5 and 5. Meanwhile, the control eggs that received 20 μL of vehicle (cremophor EL 2.5%, EtOH 2.5% in saline) and exposed to a similar light dose showed no detectable vascular alteration in the treated area. This indicated that the vascular occlusion observed in embryos treated with compound **5** was neither caused by the vehicle components nor was it thermally induced. Finally, treatment with compound **5** alone without irradiation did not induce any vascular occlusion, as nonirradiated areas remained perfused after 24 h.

As the main respiratory organ of the chick embryo, CAM is a well-vascularized membrane that is suitable as a model for PDT. It is easily accessible, inexpensive, and relatively easy to handle for photosensitizer administration, light irradiation, fluorescence analysis of administered photosensitizer, and microscopy examination of PDT-induced vascular damage.[9,17] CAM is a viable model that has been successfully used to evaluate the photodynamic-induced vascular occlusion efficacy of some photosensitizers that are in clinical trials as well as those that are already clinically

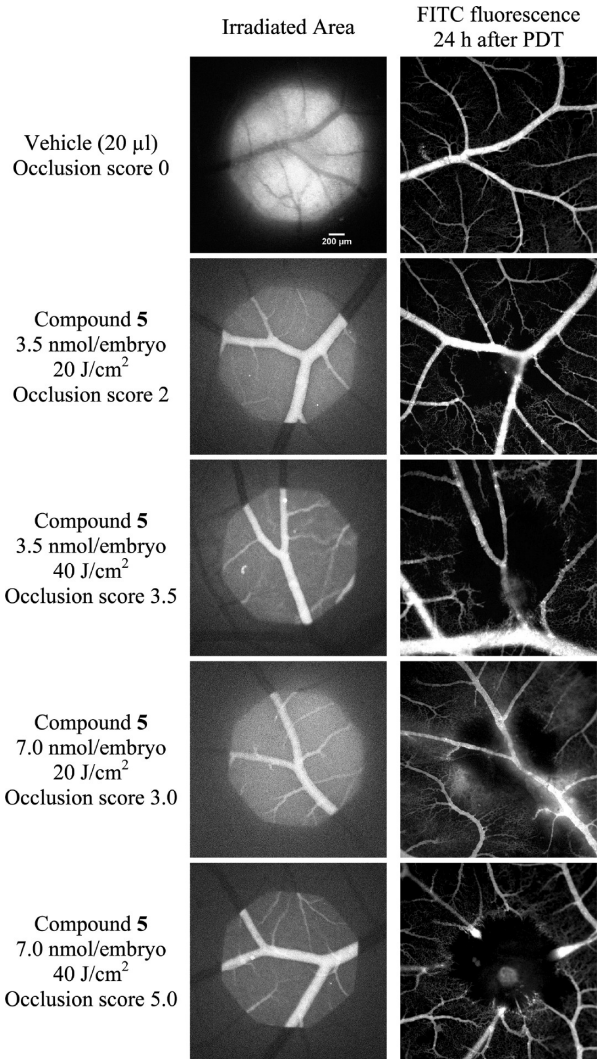

Figure 6. Representative angiographies of blood vessels supplying the CAM at beginning and 24 h after PDT, illustrating the vascular occlusion efficacy induced by compound **5** at 3.5−7 nmol/embryo. Irradiation was performed at 510−560 nm of excitation with 20−40 J/cm^2 light dose. Cremophor EL (2.5%) and EtOH (2.5%) in saline were used as a control vehicle. Objective magnification is×4.

approved such as palladium bacteriopheophorbide, porfimer sodium, lutetium texaphyrin, 5-aminolevulinic acid, and verteporfin.[18,19] For example, a PDT experiment in the CAM model using verteporfin at a dose that is similar to the recommended clinical dosage for the treatment of age-related macular degeneration has been shown to cause complete occlusion of the large neovessels, an observation that correlates well with clinical setting.[9] In addition, in a BALB/c mouse model where PDT treatment by verteporfin resulted in suppression of tumor growth, antivascular effects were also observed, whereby a decrease in the blood volume at the tumor site was noted.[20,21] The results from the study demonstrated that compound **5** was able to induce complete closure of larger vessels, which is considered favorable in PDT treatment of cancer.

Conclusions

We have demonstrated the in vitro photocytotoxic activity of BODIPY derivatives against cell lines from leukemia and two types of solid tumor. Structure−activity relationship

study indicated the importance of having iodine atoms directly substituted on the BODIPY pyrollic carbon-4 position rather than at the meso-aryl position, in accordance with the high singlet oxygen generation rate of these compounds. Extended conjugation at the 4-pyrollic positions shifts the $\lambda_{max\,abs}$ to the red but did not confer extra potency except for the compound with a single *n*-butyl acrylate ester (**12**). Hydrophilic analogues substituted with groups such as carboxylic acid, sulfonic acid, or sodium sulfonate generally drastically diminished the activity. An exception here was the doubly iodinated compound **5** with an aliphatic carboxylic acid which showed up to 100-fold lower IC_{50} value in HL-60 compared to the parent compound **1**, perhaps because of the structural difference where the carboxylic acid group is not directly conjugated with the BODIPY core. Fluorescence microscopy studies showed that compound **5** localized exclusively within the mitochondria. This, together with data from cell cycle analysis and onset of apoptosis studies, suggests that compound **5** probably induced cell death through mitochondria-dependent apoptosis rather than through damage to nucleic materials. In addition, an emulsion of compound **5** was able to occlude the vasculature network in the CAM in vivo model, further showing its potential as an effective PDT agent.

Although photosensitizers with > 600 nm excitation wavelengths allow deeper access into biological tissues for effective treatment of abnormal tissues of bigger volume, the shorter absorption wavelength of the BODIPY-based photosensitizers studied here, such as compound **5**, may be preferred in the treatment of superficial tissues. In a clinical PDT of cancer in the esophagus and bronchi with porfimer sodium II, treatment regime with light corresponding to the 514 nm excitation wavelength exhibited similar effectiveness as that with 630 nm in terms of tumor eradication but, significantly, with less damage of the deep tissue which could cause perforation in the esophagus.[22] Overall, our results suggest that BODIPY structures, especially compound **5**, have potential to be explored as a clinically useful agent for PDT of cancer.

Experimental Section

Materials. ER-Tracker Blue-White DPX, LysoTracker Blue DND-22, rhodamine 123, SYTOX Green were purchased from Molecular Probes, Invitrogen (OR). Annexin V−FITC apoptosis detection kit 1 was purchased from BD Biosciences (CA). All cell culture reagents were purchased from Gibco, Invitrogen (Auckland, New Zealand). RNase A, dimethyl sulfoxide, propidium iodide, methylene blue, 1,3-diphenylisobenzofuran, and methylthiazolyldiphenyltetrazolium bromide were purchased from Sigma (St. Louis, MO). Fluorescein isothiocyanate dextran (FITC-dextran, 20 kDa) was purchased from Sigma-Aldrich (Buchs, Switzerland). Indian ink was purchased from Pebeo S.A. (Romanel-sur-Morges, Switzerland). Cremophor EL and absolute ethanol (Fluka Biochemika, Buchs, Switzerland) were used as dosing vehicles. NaCl, 0.9%, pH 7.4 (saline), was purchased from B Braun Medical AG (Emmertbrücke, Switzerland).

Photosensitizers. The synthesis of many of the compounds studied here has already been reported elsewhere except for compounds **3**, **5**, and **7** which is shown in Scheme 1. Compound **1** was prepared using a new method whereby 3,5-dimethylpyrrole-2-carbaldehyde was treated with 1.2 equiv of $POCl_3$ followed by addition of $BF_3 \cdot OEt_2$.[23] Compound **2** was prepared from condensation of 2,4-dimethylpyrrole with 4-iodobenzene acid in $POCl_3$ and reaction of the resultant dipyrromethene intermediate with $BF_3 \cdot OEt_2$.[24] Compounds **3** and **4** were prepared from compound **2** through iodination using I_2/HIO_3 and disulfonation

Scheme 1[a]

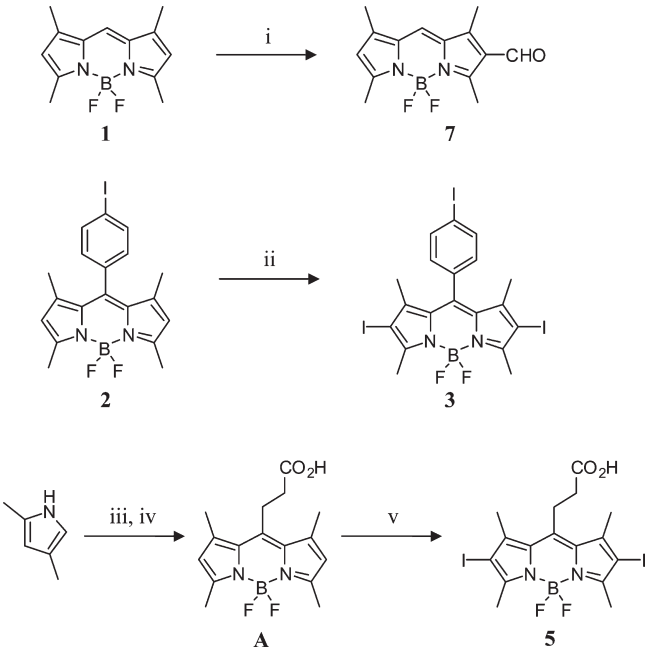

[a] Reagents and conditions: (i) $POCl_3$, DMF, 1,2-dichloroethane, 85 °C, 17 h; (ii) I_2, HIO_3, EtOH, 60 °C, 20 min; (iii) succinic anhydride, $BF_3 \cdot OEt_2$, toluene, 80 °C, 5 h; (iv) $BF_3 \cdot OEt_2$, Et_3N, 20 °C, 16 h; (v) I_2, HIO_3, MeOH, 25 °C, 30 min.

using chlorosulfonic acid,[25] respectively. Compound **5** was prepared from 2,4-dimethylpyrrole and succinic anhydride in the presence of $BF_3 \cdot OEt_2$ (to yield compound **A**), followed by iodination of the resultant BODIPY. Compound **6** was obtained from diiodination of compound **1**.[5] Compound **7** was obtained from treating compound **1** with dry dimethylformamide and $POCl_3$. Compounds **8**−**15** were prepared using palladium-catalyzed activation of the parent compound **1** using Heck-type coupling with the respective acrylate structures.[26] The experimental details for measuring the photophysical properties and synthesis of compounds **3**, **5**, and **7** are included in the Supporting Information. All compounds were dissolved in dimethyl sulfoxide (DMSO) at 10 mM, aliquoted, and stored at −20 °C prior to use.

Cells. HL-60 human promyelocytic leukemia cells were obtained from American Type Culture Collection (VA) and maintained in RPMI 1640 medium supplemented with 10% FBS. HSC-2 oral cavity human squamous carcinoma cells were obtained from Health Science Research Resources Bank (Japan Health Sciences Foundation, Japan). HK1 nasopharyngeal epithelial carcinoma cell line was a gift from University of Hong Kong Culture Collection (University of Hong Kong, Hong Kong). Both cell lines were grown in MEM medium supplemented with 10% FBS.

Photoinduced Cytotoxicity Assay. Approximately 15 000 HL-60 cells/well or 3000 cells/well for HSC-2 and HK1 cells in phenol-red-free culture medium containing 10% fetal bovine serum were seeded in a 96-well plate. HSC-2 and HK1 cells were allowed to adhere overnight before test compounds were introduced. Photosensitizer stock solutions (10 mM in DMSO) were diluted with medium, and concentrations varying from 0.001 to 100.0 μM were tested on the cells. The control wells received 0.01% of DMSO, equivalent to the highest amount of DMSO used as vehicle in the compound-treated wells. Following 2 h of treatment, cells were irradiated with a light dose of 4.1 J/cm^2 from a broad spectrum light source and fluence rate of 6.8 mW/cm^2 and were further incubated for 24 h before cell viability was assessed using MTT assay. Following incubation, 15 μL of MTT solution (5 mg/mL) was added into each well and incubated for

4 h at 37 °C. The medium was then removed, and 100 μL of DMSO was added to dissolve the formazan crystal formed. Absorbance, as a measure of viable cell number, was read at 570 nm with an OpsysMR microplate spectrometer (Thermo-Labsystems, Chantilly, VA). The dark toxicity of each photosensitizer was also determined in every experiment.

Comparative Singlet-Oxygen Generation Measurements. An amount of 8 mL of aerated isopropanol containing 50 μM of DPBF and the photosensitizer (0.5 μM or 5 μM) in a 6-well plate was irradiated at 6.8 mW/cm^2 of filtered light source of >510 nm wavelength with a Roscolux medium yellow no. 10 filter (Rosco, NY) at room temperature for 1 h. Aliquots of 200 μL were removed from the mixture at various fixed intervals, and the absorbance was measured at 410 nm. The rate of singlet oxygen production was determined from the reduction in intensity of absorbance recorded over time. Irradiation of DPBF−isopropanol solution in the absence of photosensitizer as a negative control and solution containing methylene blue as a comparative control was also carried out. The relative singlet oxygen generation rate for each of the photosensitizers was determined by using methylene blue as a reference.

Cellular Localization. HSC-2 cells grown on round glass coverslips in 12-well plates were co-incubated with 100 nM photosensitizer together with organelle-specific fluorescence probes. The endoplasmic reticulum was labeled with 100 nM of ER-Tracker Blue-White DPX, the lysosomes were stained with 500 nM of LysoTracker Blue DND-22, and the mitochrondria were tracked with 100 nM Rh123, each for 15−30 min of incubation at room temperature. After incubation, cells were gently rinsed in PBS to remove free dyes, and the stained cells were observed using Olympus DSU spinning disk confocal microscope configured with a PlanApo 63× oil objective (Olympus Optical Corp. Ltd., Tokyo, Japan) and iXon EM + digital camera (Andor Technology, South Windsor, CT). Fluorescent images of *XY* sections at 0.2 μm were collected sequentially using Olympus Cell software. Organelle-specific fluorescence probes were respectively excited at 330−385 nm wavelengths to illuminate ER-tracker and LysoTracker, at 460−490 nm for Rh123 and at 520−550 nm for the photosensitizer.

Annexin V−FITC Apoptosis Analysis. HSC-2 cells grown in 60 mm dishes at 50% confluency were treated with 0.5 μM compound **5**. Following 2 h of incubation, cells were irradiated with 4.1 J/cm^2 of broad spectrum light. At various treatment intervals, floating cells in the medium were pooled together with the adherent cells after trypsinization and were washed twice with cold phosphate buffered saline (PBS). The cells were resuspended with 1× binding buffer at 1×10^6 cells/mL. A 100 μL of cell suspension was transferred to a flow cytometry tube followed by 5 μL of annexin V−FITC and 5 μL of 200 μg/mL propidium iodide in PBS. The cells were gently mixed and incubated for 15 min at room temperature in the dark before analysis on a FACSCalibur flow cytometer equipped with a 488 nm argon laser. The fluorescence data of 1×10^4 cells were collected with the FL1 detector with 530/30 band-pass filter to collect annexin−FITC fluorescence and with the FL3 detector with a 630 nm long-pass filter to collect propidium iodide fluorescence.

Cell Cycle Analysis. HSC-2 cells were treated with 0.25 μM compound **5** and collected as above. Cells were then fixed in 70% ice-cold ethanol (v/v in PBS) overnight at 4 °C. Following fixation, the cells were washed twice in cold PBS. The pellet was then resuspended in PBS solution containing 20 μg/mL RNase A and 1 μM SYTOX Green for 30 min. The cells were analyzed on a FACSCalibur flow cytometer with 488 nm argon laser. The DNA−SYTOX Green fluorescence of 1×10^4 cells were collected with the FL1 detector with 530/30 band-pass filter.

PDT on the CAM Vasculature (in Ovo). Freshly obtained fertilized chicken eggs were incubated with the narrow apex down in a 90° swinging incubator (Savimat MG 200, Chauffry, France) at 37 °C and 65% relative humidity. On embryo development day (EDD) 3, an opening on the eggshell, about 4 mm in diameter, was bored at the apex and sealed with adhesive tape to avoid contamination and desiccation of the egg contents. The eggs were further incubated in stationary position with the apex upright until EDD-9.

Microscopic observation of CAM vasculature and the light irradiation during PDT were performed with an epifluorescence Eclipse 600 FN microscope equipped with a CFI Achromat 4×/0.1 objective (Nikon, Japan). Illumination was provided by a 100 W mercury arc lamp (Osram, GmbH, Augsburg, Germany). Light doses were adjusted with neutral density filters and measured with a calibrated Field-Master GS power analyzer (Coherent, Santa Clara, CA). For exciting and detecting compound **5**, the microscope was equipped with a G-2A filter set (excitation, 510−560 nm) (Nikon, Japan). For detecting FITC, a B-2E/C filter set (excitation, 465−495 nm) was used (Nikon, Japan). Fluorescence angiograms (1280 × 1024 pixels with 4095 gray level, i.e., 12 bits) were acquired with an F-view II 12-bit monochrome Peltier-cooled digital CCD camera driven with analySIS DOCU software from Soft Imaging System (Münster, Germany). The fluorescence images were stored in a 16-bit TIF file.

On EDD-9, the egg opening was extended to ∼30 mm in diameter. Embryo was intravenously administered with a single bolus of 3.5−7 nmol/embryo of photosensitizer in dosing vehicle (cremophor EL 5%, EtOH 5% in saline) at the CAM main vasculature. A minute after injection, a site with vessels of diameter between 5 and 100 μm was irradiated at a light dose of 20−40 J/cm^2 filtered at 510−560 nm with an irradiation area of 0.02 cm^2 and fluence rate of 40 mW/cm^2. The site was photographed at the beginning and at the end of irradiation. Subsequently, the egg opening was sealed with parafilm and the embryo was further incubated for 24 h before assessing the PDT damage induced.

Fluorescence angiograms were performed in order to assess the PDT-induced vasculature damage. Blood vessels were perfused with 10 μL of 25 mg/mL FITC−dextran followed by injection of Indian ink in order to decrease the embryo's interfering fluorescence from deeper located vessels. This interfering luminescence may change rapidly with time because of the embryo's movement. Prior to injection, the Indian ink was filtered using a sterile cellulose acetate membrane (0.2 μm pores, Renner GmbH, Darmstadt, Germany). The vasculature network at the site of irradiation was illuminated by exciting the FITC at 465−495 nm wavelengths on the epifluorescence microscope. The vasculature network was imaged, and the damage induced by PDT was scored according to the criteria as defined by Lange et al. (Table 1).[8] At least 10 embryos were assessed for each treatment group.

Acknowledgment. This work was supported by grants from the Cancer Research Initiatives Foundation. We thank David Lyn (Matrix Optics, Malaysia) for help with the cellular localization experiments.

Note Added after ASAP Publication. This paper was published on March 3, 2010 with an error in the O'Shea structure. The revised version was published on March 8, 2010.

Supporting Information Available: General procedures for spectroscopic measurements, synthesis procedures, and characterization data for compounds **1**−**15**. This material is available free of charge via the Internet at http://pubs.acs.org.

References

(1) Allison, R. R.; Downie, G. H.; Cuenca, R.; Hu, X. H.; Childs, C. J. H.; Sibata, C. H. Photosensitizers in clinical PDT. *Photodiagn. Photodyn. Ther.* **2001**, *1*, 27–42.
(2) Dolmans, D. E.; Fukumura, D.; Jain, R. K. Photodynamic therapy for cancer. *Nat. Rev. Cancer* **2003**, *3*, 380–387.

(3) Hopper, C. Photodynamic therapy: a clinical reality in the treatment of cancer. *Lancet Oncol.* **2000**, *1*, 212–219.
(4) Nyman, E. S.; Hynninen, P. H. Research advances in the use of tetrapyrolic photosensitizers for photodynamic therapy. *J. Photochem. Photobiol., B* **2004**, *73*, 1–28.
(5) Yogo, T.; Urano, Y.; Ishitsuka, Y.; Maniwa, F.; Nagano, T. Highly efficient and photostable photosensitizer based on BODIPY chromophore. *J. Am. Chem. Soc.* **2005**, *127*, 12162–12163.
(6) Gorman, A.; Killoran, J.; O'Shea, C.; Kenna, T.; Gallagher, W. M.; O'Shea, D. F. In vitro demonstration of the heavy-atom effect for photodynamic therapy. *J. Am. Chem. Soc.* **2004**, *126*, 10619–10631.
(7) Byrne, A. T.; O'Connor, A. E.; Hall, M.; Murtagh, J.; O'Neill, K.; Curran, K. M.; Mongrain, K.; Rousseau, J. A.; Lecomte, R.; McGee, S.; Callanan, J. J.; O'Shea, D. F.; Gallagher, W. M. Vascular-targeted photodynamic therapy with BF2-chelated tetraaryl-azadipyrromethene agents: a multi-modality molecular imaging approach to therapeutic assessment. *Br. J. Cancer* **2009**, *101*, 1565–1573.
(8) Atilgan, S.; Ekmekci, Z.; Dogan, A. L.; Guc, D.; Akkaya, E. U. Water soluble distyryl-boradiazaindacenes as efficient photosensitizers for photodynamic therapy. *Chem. Commun.* **2006**, *42*, 4398–4400.
(9) Lange, N.; Ballini, J. P.; Wagnières, G.; van den Bergh, H. A new drug screening procedure for photosensitizing agents used in photodynamic therapy for CNV. *Invest. Ophthalmol. Visual Sci.* **2001**, *42*, 38–46.
(10) Burghart, A.; Kim, H.; Welch, M. B.; Thoresen, L. H.; Reibenspies, J.; Burgess, K. 3,5-Diaryl-4,4-difluoro-4-bora-3a,4a-diaza-*s*-indacence (BODIPY) dyes: synthesis, spectroscopic, electrochemical, and structural properties. *J. Org. Chem.* **1999**, *64*, 7813–7819.
(11) Kochevar, I. E.; Redmond, R. W. Photosensitized production of singlet oxygen. *Methods Enzymol.* **2000**, *319*, 20–28.
(12) McBride, H. M.; Neuspiel, M.; Wasiak, S. Mitochodria: more than just a powerhouse. *Curr. Biol.* **2006**, *16*, R551–R56.
(13) Morgan, J.; Oseroff, A. R. Mitochondria-based photodynamic anti-cancer therapy. *Adv. Drug Delivery Rev.* **2001**, *49*, 71–86.
(14) Vantiegham, A.; Xu, Y.; Assefa, Z.; Piette, J.; Vandenheede, J. R.; Merlevede, W.; de Witte, P. A. M.; Agostinis, P. Phosphorylation of Bcl-2 in G_2/M phase-arrested cells following photodynamic therapy with hypericin involves a CDK1-mediated signal and delays the onset of apoptosis. *J. Biol. Chem.* **2002**, *277*, 37718–37731.
(15) Lee, H. B.; Ho, A. S. H.; Teo, S. H. p53 status does not affect photodynamic cell killing induced by hypericin. *Cancer Chemother. Pharmacol.* **2005**, *58*, 91–98.
(16) Chen, B.; Pogue, B. W.; Hoopes, P. J.; Hasan, T. Vascular and cellular targeting for photodynamic therapy. *Crit. Rev. Eukaryotic Gene Expression* **2006**, *16*, 276–305.
(17) Vargas, A.; Zeisser-Labouébe, M.; Lange, N.; Gurny, R.; Delie, F. The chick embryo and its chorioallantoic membrane (CAM) for the in vivo evaluation of drug delivery systems. *Adv. Drug Delivery Rev.* **2007**, *59*, 1162–1176.
(18) Rück, A.; Böhmler, A.; Steiner, R. PDT with TOOKAD studied in the chorioallantoic membrane of fertilized eggs. *Photodiag. Photodyn. Ther.* **2005**, *2*, 79–90.
(19) Hammer-Wilson, M. J.; Cao, D.; Kimel, S.; Berns, M. W. Photodynamic parameters in the chick chorioallantoic membrane (CAM) bioassay for photosensitizers administered intraperitoneally (IP) into the chick embryo. *Photochem. Photobiol. Sci.* **2002**, *1*, 721–728.
(20) Ichikawa, K.; Takeuchi, Y.; Yonezawa, S.; Hikita, T.; Kurohane, K.; Namba, Y.; Oku, N. Antiangiogenic photodynamic therapy (PDT) using Visudyne causes effective suppression of tumour growth. *Cancer Lett.* **2004**, *205*, 39–48.
(21) Kurohane, K.; Tominaga, A.; Sato, K.; North, J. R.; Namba, Y.; Oku, N. Photodynamic therapy targeted to tumour-induced angiogenic vessels. *Cancer Lett.* **2001**, *167*, 49–56.
(22) Grosjean, P.; Wagnieres, G.; Fontolliet, C.; van den Bergh, H.; Monnier, P. Clinical photodynamic therapy for superficial cancer in the oesophagus and the bronchi: 514 nm compared with 630 nm light irradiation after sensitization with photofrin II. *Br. J. Cancer* **1998**, *77*, 1989–1995.
(23) Wu, L.; Burgress, K. A new synthesis of symmetric boraindacene (BODIPY) dyes. *Chem. Commun.* **2008**, *40*, 4933–4935.
(24) Tahtaoui, C.; Thomas, C.; Rohmer, F.; Klotz, P.; Duportail, G.; Mély, Y.; Bonnet, D.; Hibert, M. Convenient method to access new 4,4-dialkoxy- and 4,4-dialkoxy-diaza-*s*-indacene dyes: synthesis and spectroscopic evaluation. *J. Org. Chem.* **2007**, *72*, 269–272.
(25) Li, L.; Han, J.; Nguyen, B.; Burgess, K. Synthesis and spectral properties of functionalized, water-soluble BODIPY derivatives. *J. Org. Chem.* **2008**, *73*, 1963–1970.
(26) Thivierge, C.; Bandichhhor, R.; Burgess, K. Spectral dispersion and water solubilization of BODIPY dyes via palladium-catalyzed C−H functionalization. *Org. Lett.* **2007**, *9*, 2135–2138.